Transportation Research Part C 149 (2023) 104062

Contents lists available at ScienceDirect

Transportation Research Part C

journal homepage: www.elsevier.com/locate/trc

# Pricing lane changes

Ang Ji [a,b,*], Mohsen Ramezani [b], David Levinson [b]

[a] School of Transportation and Logistics, Southwest Jiaotong University, Chengdu, China
[b] School of Civil Engineering, The University of Sydney, Sydney, Australia

ARTICLE INFO

*Keywords:*
Lateral dynamics
Game theory
Road pricing
Micro-toll

ABSTRACT

Risky and aggressive lane changes on highways reduce capacity and increase the risk of collision. We propose a lane-changing pricing scheme as an effective tool to penalize those maneuvers to reduce congestion as a societal goal while aiming for safe driving conditions. In this paper, we first model driver behavior and their payoffs under a game theory framework and find optimal lane-changing strategies for individuals and their peers in multiple pairwise games. Payoffs are estimated for two primary evaluation criteria: efficiency and safety, which are quantified by incorporating driver tradeoffs. After that, the discretionary lane-changing (DLC) model is calibrated and validated by real-world vehicular trajectory data. To manipulate drivers' DLC behaviors, two types of lane-changing tolls based on local-optimal and global-optimal rules are introduced to align individual preferences with social benefits. We find prices can close this gap and achieve 'win-win' results by reducing drivers' aggressive lane changes in the congested traffic. Meanwhile, the tolls collected can be used to compensate drivers who get delayed when yielding, to encourage appropriate yielding behavior and a pseudo-revenue neutral tolling system.

## 1. Introduction

Lane changing (LC) in traffic occurs often, and is a major source of road crashes and traffic congestion at merge bottlenecks (Jula et al., 2000; Coifman et al., 2006; Laval and Daganzo, 2006; Pande and Abdel-Aty, 2006; Li et al., 2020). Lane changing/merging accounted for 5.3% of all police-reported motor vehicle crashes in the United States in 2019, and resulted in about 1.8% of incapacitating injuries (National Highway Traffic Safety Administration, 2021). Meanwhile, it is found that lane changes can trigger road capacity reductions and traffic oscillations (Patire and Cassidy, 2011; Cassidy and Rudjanakanoknad, 2005; Mauch and Cassidy, 2002). A recent study also reveals that a single discretionary LC behavior delays 4–5 surrounding vehicles, and the impact duration is up to 12–13 s (He et al., 2022). When vehicles change lanes in congested traffic states, they simultaneously occupy space in two lanes. Lane changing is over-consumed because lane changers do not suffer the full cost they impose on other travelers. Motorists then drive and change lanes more frequently because of the low personal cost. In general, drivers need discretionary lane changes (DLCs) to gain a speed advantage or execute mandatory lane changes (MLCs) to enter or exit highways. All else equal, when changing lanes, they appreciate the yielding of other drivers, while they prefer not to yield themselves (Ji et al., 2022).

Most conventional microscopic LC models (e.g. acceleration models, MOBIL model, MITSIM model, gap-acceptance model, etc.) focus on safe and reasonable lane changes from the users' view (Gipps, 1986; Hidas, 2005; Toledo et al., 2003). In contrast, macroscopic models describe LC behaviors as filling vacant gaps in a continuous fluid-like traffic flow (Lighthill and Whitham, 1955; Richards, 1956; Jin, 2010; Ramezani and Ye, 2019). From a different perspective, the LC maneuver can be regarded as a

* Corresponding author at: School of Transportation and Logistics, Southwest Jiaotong University, Chengdu, China.
*E-mail addresses:* ang.ji@swjtu.edu.cn (A. Ji), mohsen.ramezani@sydney.edu.au (M. Ramezani), david.levinson@sydney.edu.au (D. Levinson).

https://doi.org/10.1016/j.trc.2023.104062
Received 5 June 2022; Received in revised form 13 February 2023; Accepted 15 February 2023

**Nomenclature**

| | |
|---|---|
| $\Delta\tau$ | Net revenue of micro-pricing scheme |
| $\Delta v_{i,j}$ | Speed difference between two vehicles $i$ and $j$ |
| $\Delta x_{i,j}$ | Distance gap between two vehicles $i$ and $j$ |
| $\delta$ | Jam spacing |
| $\lambda$ | Reaction time |
| $\mathbb{M}, \mathbb{F}$ | Strategy sets of M and F: ($c$ for change lanes, $s$ for stay in the current lane); ($n$ for not yield, $y$ for yield) |
| $\mathbf{M_e}$ | A mass-related parameter in the ELVIS model |
| $\mathrm{VOT_z}$ | Value of Time |
| $\Phi_1, \Phi_2$ | Best-response polytopes in $2 \times 2$ matrix of LC games |
| $\psi$ | Trade-off ratio between safety costs and speed benefits |
| $\tau$ | Micro-pricing profile |
| $\tau_{\mathrm{P}}$ | Penalty given to aggressive lane-changing behaviors |
| $\tau_{\mathrm{R}}$ | Reward compensated to yielding actions of F |
| $\theta$ | Conversion factor of the statistical value of life according to different levels of Maximum Abbreviated Injury Scores |
| $\varepsilon$ | Error term that captures unobserved effects |
| $a$ | Acceleration rate |
| $C_{\mathrm{NE}}, C_{\mathrm{LO}}$ | Payoff at Nash Equilibrium or Local Optimization |
| $C_{\mathrm{total},z}$ | Total payoff for player $z$ |
| $C_t$ | Summation of payoffs in one strategy pair |
| $E_z$ | Expected payoff of vehicle $z$ |
| $i, I$ | Lane ID from 1 being the left-most lane to the right-most lane $I$ |
| $k, K$ | LC game pair from 1 to $K$ in the whole system |
| $N$ | Number of vehicles in a selected lane |
| $P', Q'$ | Global Optimality strategy profile |
| $p, q$ | Probabilities that drivers behave to defect |
| $P^*, Q^*$ | Nash Equilibrium strategy profile |
| $P^o, Q^o$ | Pareto (Local) Optimality strategy profile |
| $S_z$ | Safety cost for player $z$ |
| $s_{\mathrm{p}}, s_{\mathrm{s}}$ | Safety proximity/severity indicators |
| $v^{\mathrm{d}}$ | Desired speed |
| $V_{\mathrm{z}}$ | Speed benefit obtained by player $z$ |
| $v_0$ | Initial speed before the LC game starts |
| $x$ | Longitudinal position of vehicles |
| $Y$ | Energy-based function in ELVIS model |
| $z$ | Indicator for vehicles participating in the LC game |
| M, F, L | The subject merging vehicle, its opponent vehicle, and the lead vehicle in the receiving lane |

strategic interaction where drivers compete or cooperate. Game theory (GT), developed by Von Neumann and Morgenstern (1944), provides insights to understand interactions among multiple agents. It has wide application in recent transport studies (Littlechild and Thompson, 1977; Bell, 2000; Chen et al., 2018; Fisk, 1984; Ji and Levinson, 2020c), which complements the advantages of microscopic and macroscopic models and allows consideration of interactive behaviors. Although the LC maneuver is complicated in the real world, we argue modeling with simple rules of game theory helps reveal how drivers make decisions under different conditions and build on it to develop micro-pricing of LC to manipulate the frequency of lane changes.

The interaction among drivers can be described as a multi-player game, in which players (arguably) rationally adopt strategies based on how others behave. However, in some cases, their preferences may conflict with the mutually beneficial outcome, which causes a social dilemma wherein players make personally rational but socially costly choices. The present paper develops solutions to reduce or mitigate the dilemma.

To foster cooperative strategies among players, some studies propose reciprocity, such as direct and indirect mechanisms, by introducing Evolutionary Game Theory (EGT) (Cortés-Berrueco et al., 2016; Iwamura and Tanimoto, 2018). According to reciprocity, people are encouraged to cooperate after being recognized over repeated games. The EGT approach induces social identity for players to reduce the negative effect of the social dilemma. Because we cannot count on repeated encounters on the road between the same players in DLC maneuvers, we test externally-imposed enforcement (i.e. micro-pricing) to motivate cooperation among stranger drivers and demotivate socially detrimental behaviors.

**Table 1**
Summary of studies on game theory-based cooperative lane-changing.

| Study | Scale | Method | LC types | Utility | Validation |
|---|---|---|---|---|---|
| Lou et al. (2011) | Macro | Tolls for HOV/HOT lanes | DLC | Overall traffic efficiency | Simulation |
| Wang et al. (2015) | Micro | Cooperative cost term | DLC | Safety, equilibrium, control, efficiency, route, lane preference, and lane switch | Simulation |
| Cortés-Berrueco et al. (2016) | Macro | Nowak's mechanisms (Nowak, 2006) | DLC | Space advantages and safe distances | Simulation |
| Iwamura and Tanimoto (2018) | Macro | Replicator dynamics | DLC | Space advantages and safe distances | Simulation |
| Zimmermann et al. (2018) | Macro | Virtual benefits and sanctions | DLC | Time gain, loss, and pressure | Driver simulator |
| Kang and Rakha (2018) | Micro | Repeated game and accumulated payoffs | MLC | Expected gap and relative speed | Simulation |
| Ali et al. (2019) | Micro | Connected environment | MLC | Speed variations and safety costs | Driver simulator |
| Lin et al. (2019) | Micro | Utility transfer | DLC | Time and safety costs | Simulation |
| This paper | Micro & Macro | Pricing schemes | DLC | Speed advantages and safety costs | Simulation |

Road pricing provides a possible solution for prompting cooperation, regarded as an effective social cost-minimizing mechanism (Levinson, 2005). It is designed to internalize negative externalities, aiming to increase road capacity and safety by aligning individual decision-making with social welfare. However, to date, road pricing strategies have been relatively macroscopic in nature and have aimed to regulate the presence of a vehicle in the network by general location or time, but not the maneuver dynamics of individual vehicles. The effect of pricing strategy on traffic oscillations caused by lane changes (microscopic behaviors) remains undetermined. Some similar insights were proposed by Lin et al. (2019) and Zimmermann et al. (2018) with utility transaction or virtual rewards designed in games, but which have yet to be specified as exact pricing schemes (see Table 1 for comparisons). The need for penalizing aggressive DLC serves as the motivation of this study.

In this paper, we propose a micro-pricing method to penalize socially-detrimental lane changes based on the local-optimal (LO) approach (microscopic scale) or the global-optimal (GO) approach (macroscopic scale) and compare their effects. This pricing does not aim to prevent intended lane changes strictly, but to engage public-good driving behaviors and incentivize drivers to consider the social consequences (delay or risk experienced by others) in their decision.

The main contribution of this study includes developing a DLC behavior paradigm to model the trade-off between safety and efficiency in real values. Furthermore, unlike existing road tolls, the proposed LC pricing focuses on micro-interactions. Besides, the proposed model and pricing schemes are tested through a microsimulation environment to examine their performance with various traffic demands.

The paper is structured as follows. In Section 2, a simultaneous two-player game theory LC model is first established and analyzed to discover drivers' possible strategies and corresponding payoffs in LC games. From both microscopic and macroscopic perspectives, Section 3 proposes the possible improvements for LC games with the potential conflict of interests. Based on those optimization solutions, we apply two types of pricing rules to eliminate the social dilemma. Next, in Section 4, the model calibration and validation process are first conducted to capture human naturalistic driving behavior from real-world trajectories. It is then followed by the performance of pricing schemes in simulated experiments, and finally, the simulation results are presented in Section 5. In Section 6, model applicability and potential improvements are summarized and discussed.

## 2. Two-player non-cooperative LC game

### *2.1. Basic assumptions*

Modeling LC with game theory requires several simplifying assumptions. First, players (i.e., drivers) are assumed to be rational and aim to best satisfy their own preferences (in this game to maximize their individual payoffs), under the circumstance of understanding others are also rational. That is, nobody will doubt the actions of others.

Second, we assume each player follows the same game rules and has all related information, which includes all possible strategies and payoffs. The assumption of complete and perfect information exists throughout the whole game. That enables players to make decisions recognizing others' possible moves. We assume players achieve this by perceiving not only their own situation in their current *subject* lane, but the situation of vehicles in the prospective *receiving* lane.

Last, we specify the payoffs of drivers in LC games considering speed benefits and safety costs. Players trade-off 'greed' and 'fear' to find the best balance, which means they desire to obtain speed benefits while avoiding paying in terms of risk. This 'trade-off' will be quantified by payoffs, which are also known to all players, introduced in the next section.

### *2.2. Players and strategies*

Drivers may adopt various strategies and actions during the driving task. We assume the simplest case where two players are involved in LC: the vehicle that plans to change (merge) to the receiving lane (M) and the vehicle immediately following in the receiving lane (F), as demonstrated in Fig. 1. (We use the terms *driver*, *player*, and *vehicle* interchangeably hereafter). To simplify, Vehicle M can either change lanes ('c') or choose to stay and wait ('s'), while Vehicle F responds by yielding ('y') or not yielding ('n') to that LC decision. Therefore, we define the feasible strategy sets for M ($\mathbb{M} = \{c, s\}$) and for F ($\mathbb{F} = \{n, y\}$). The behavior of M and F will also be influenced by the position and the speed of the lead vehicle (L) in the receiving lane. In the following, we try to define these behaviors by referring to only trajectories. We assume the game between the two players starts within a fairly close distance (e.g. 50 m), so they can observe the specific actions and interact with each other.

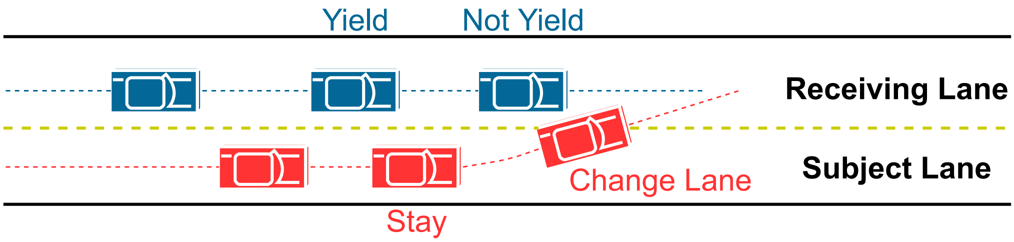


**Fig. 1.** Two-player LC game diagram (Vehicle M in red interacts with Vehicle F in blue, Vehicle L in green serves as a third party).

### 2.3. Driver payoff function

In the proposed game-theoretic model, short-run speed (travel time) benefits and safety costs (defined as non-negative), denoted as $V$ and $S$, are considered. It is assumed that the two players equally incur the safety cost when a crash occurs, while speed benefits differ according to their strategy and individual expected travel speed. Benefits over the long run will not be discussed due to the difficulties of evaluation and quantification.

#### 2.3.1. Speed benefits

The speed benefit considers the advantage of travel time savings by expected driving speeds. The time-advantageous strategies, including changing lanes ('c') and not yielding ('n'), motivate drivers to catch up with the vehicle driving ahead, while the courteous strategies suffer from slower speeds. If Vehicle M changes lanes, it will drive at the expected speed perhaps profiting from this decision. Otherwise, Vehicle M needs to tolerate the low speed following the current slow-moving leader.

If Vehicle F decides to give way (yield), it will allow Vehicle M to cut in and then assume the role of its leader in the target lane. In contrast, in the no yield case, Vehicle F tailgates its previous leader under the assumption that Vehicle M will finally give up changing due to its blockage. Therefore, the speed benefit of F depends on whether M changes lanes or not, and the change in spacing between Vehicle F and its new (or old) leader. The speed payoffs for all combinations of strategies are presented in Eq. (1). Note a constant term is added to the payoff function to capture the preferences in different strategies.

$$V_{\mathrm{M}}(c,n) = V_{\mathrm{M}}(c,y) = \beta_{11} + \beta_{12}(v^{\mathrm{d}}_{\mathrm{M}}(\Delta x_{\mathrm{LM}}) - v_{\mathrm{M}}) \tag{1a}$$

$$V_{\mathrm{M}}(s,n) = V_{\mathrm{M}}(s,y) = 0 \tag{1b}$$

$$V_{\mathrm{F}}(n,c) = \beta_{21} + \beta_{22}(v^{\mathrm{d}}_{\mathrm{F}}(\Delta x_{\mathrm{LF}}) - v_{\mathrm{F}}) \tag{1c}$$

$$V_{\mathrm{F}}(n,s) = 0 \tag{1d}$$

$$V_{\mathrm{F}}(y,c) = V_{\mathrm{F}}(y,s) = \beta_{31}(v^{\mathrm{d}}_{\mathrm{F}}(\Delta x_{\mathrm{MF}}) - v_{\mathrm{F}}) \tag{1e}$$

in which $V_{\mathrm{M}}$ and $V_{\mathrm{F}}$ are speed benefits of Vehicle M and F (for example, $V_{\mathrm{M}}(c,n)$ denotes the speed payoff of Vehicle M if it performs 'c' (change lane) and Vehicle F performs 'y' (yielding)), $\beta_{12}$, $\beta_{22}$, and $\beta_{31}$ are coefficients to be estimated, $\beta_{11}$ and $\beta_{21}$ are constants that capture the driver preference on aggressive strategies to gain more benefits, $\Delta x_{\mathrm{LM}}$, $\Delta x_{\mathrm{LF}}$, and $\Delta x_{\mathrm{MF}}$ are relative positions or front-to-front spacing (1) between Vehicle M and its new leader L (on the receiving lane); (2) between Vehicle F and its current leader L; and (3) between Vehicle F and M, and $v_{\mathrm{M}}$ and $v_{\mathrm{F}}$ are the instantaneous speeds of Vehicles M and F, respectively.

In this paper, we resort to the method proposed in Wang et al. (2015), assuming that vehicles expect to drive at the free-flow speed $v_{\mathrm{f}}$ when no vehicles are ahead while adopting the appropriate speed to safely follow the existing leader. We assume the desired speed $v^{\mathrm{d}}$ is a function of front to front spacing with the (potential) leader vehicle.

$$v^{\mathrm{d}}(\Delta x) = \begin{cases} v_{\mathrm{f}} & \Delta x > \Delta x_{\mathrm{f}} \\ \frac{\Delta x - \Delta x_0}{t^{\mathrm{d}}} & \Delta x \le \Delta x_{\mathrm{f}} \end{cases} \tag{2}$$

where $\Delta x$ is the front-to-front spacing between the subject vehicle and its leader, $v_{\mathrm{f}}$ is the free-flow speed, $\Delta x_{\mathrm{f}}$ is a gap threshold ($= v_{\mathrm{f}}t^{\mathrm{d}} + \Delta x_0$), $t^{\mathrm{d}}$ denotes the desired time headway, and $\Delta x_0$ represents the minimum safe gap.

Speed benefits can be rather small for DLCs, while it becomes more significant for MLCs. If drivers fail to execute MLCs, they face a high cost. Because of their unsuccessful attempts for MLCs, they may need to complete a severe braking maneuver or even a complete stop to wait for available gaps, otherwise, they will spend more time making U-turns and backtracking to their expected destination. This significant loss induces a stronger motivation to take risks in mandatory situations than DLCs. We will leave the discussion for MLCs to future studies.

#### 2.3.2. Safety costs

The safety cost $S$ is estimated by the potential risk of collision. It is estimated from two perspectives: proximity and severity. Previous studies focus on the proximity to a crash and exploit surrogate measures (like Time-to-Collision (TTC) in Kita, 1999,

**Table 2**
Relative disutility factors for injuries based on quality-adjusted life year (QALY) studies (Spicer and Miller, 2010).

| MAIS level | Severity | Fraction of VSL ($\theta$) |
|---|---|---|
| Level 1 | Minor | 0.003 |
| Level 2 | Moderate | 0.047 |
| Level 3 | Serious | 0.105 |
| Level 4 | Severe | 0.266 |
| Level 5 | Major | 0.593 |
| Level 6 | Fatality | 1.000 |

deceleration to prevent a collision in Talebpour et al., 2015, and Post-Encroachment Time (PET) in Ali et al., 2018) to assess the safety by conflicts.

Recent works extend the safety assessment to include the severity as well (Sobhani et al., 2011; Laureshyn et al., 2017; Ji and Levinson, 2020a). Crash severity may depend on several factors, typically analyzed by statistical regression. Then, the safety cost from potential crashes can be estimated by the product of the probability of conflicts, the probability of severe injuries, and the adjusted value of a statistical life ($\theta * \mathrm{VSL}$) based on different levels of Maximum Abbreviated Injury Scores (MAIS). The conversion table between the injury severity and the VSL is given in Table 2.

$$S(\Delta x, \Delta v) = s_{\mathrm{p}}(\Delta x, \Delta v) \cdot s_{\mathrm{s}}(\Delta v) \cdot \theta(\mathrm{MAIS}) \cdot \mathrm{VSL} \tag{3a}$$

$$s_{\mathrm{p}}(\Delta x, \Delta v) = \exp\left[-\left(\frac{\mathrm{TTC}(\Delta x, \Delta v)^2}{2R^2}\right)\right]; \quad s_{\mathrm{s}}(\Delta v) = \frac{1}{1+\exp(-Y(\Delta v, \mathbf{M_e})} \tag{3b}$$

$$\frac{\partial S}{\partial \Delta x} = \left(-\frac{\Delta x}{\Delta v^2 R^2}\right) \cdot s_{\mathrm{p}} \cdot s_{\mathrm{s}} \cdot \theta \cdot \mathrm{VSL} < 0 \tag{3c}$$

$$\frac{\partial S}{\partial \Delta v} = \left(\frac{\Delta x^2}{\Delta v^3 R^2} + 2\mathbf{M_e}\Delta v \ln s_{\mathrm{s}}\right) \cdot s_{\mathrm{p}} \cdot s_{\mathrm{s}} \cdot \theta \cdot \mathrm{VSL} > 0 \tag{3d}$$

$$Y = 0.5 \cdot \mathbf{M_e} \Delta v^2 \cdot (1 - e^2) \tag{3e}$$

where $s_{\mathrm{p}}$ and $s_{\mathrm{s}}$ represent the crash proximity and severity respectively, $\Delta x$ is the distance gap between the two vehicles, $\Delta v$ is the relative speed of the two vehicles ($\Delta v = v_{\mathrm{follower}} - v_{\mathrm{leader}}$), $\theta$ is the adjusted ratio of VSL by different levels of MAIS in a possible crash, TTC is the safety indicator Time-to-collision and its threshold is set as 1.5 s to distinguish risky conditions from safe ones (Gettman et al., 2008; Society of Automotive Engineers, 2015), $R$ is the scaling coefficient to be calibrated, $Y$ is an energy-based function in the ELVIS model (see Ji and Levinson, 2020a for more information), with corresponding thresholds and coefficients for each level of MAIS, and $\mathbf{M_e}$ and $e$ are a mass-related parameter and the coefficient of restitution in the ELVIS model. Distances $\Delta x$ and relative speeds $\Delta v$ vary between any two vehicles, and a small $\Delta x$ or a large $\Delta v$ increases the safety cost.

Then, the safety cost of Vehicle M ($S_{\mathrm{M}}$) and F ($S_{\mathrm{F}}$) with different strategy combinations can be estimated as:

$$S_{\mathrm{M}}(c, n) = S_{\mathrm{M}}(c, y) = S(\Delta x_{\mathrm{MF}}, \Delta v_{\mathrm{MF}}) + S(\Delta x_{\mathrm{LM}}, \Delta v_{\mathrm{LM}}) \tag{4a}$$

$$S_{\mathrm{M}}(s, n) = S_{\mathrm{M}}(s, y) = 0 \tag{4b}$$

$$S_{\mathrm{F}}(n, c) = S_{\mathrm{F}}(y, c) = S(\Delta x_{\mathrm{MF}}, \Delta v_{\mathrm{MF}}) \tag{4c}$$

$$S_{\mathrm{F}}(n, s) = S_{\mathrm{F}}(y, s) = S(\Delta x_{\mathrm{LF}}, \Delta v_{\mathrm{LF}}) \tag{4d}$$

Note that, for simplification, this study investigates three vehicles (M, F, and L) in LC maneuvers, which is consistent with most studies considering the gap acceptance in the receiving lane. When changing lanes, Vehicle M needs to consider its relative position and speed with both Vehicle F and L to avoid collisions, so two cost terms are included in Eq. (4a).

#### 2.3.3. Overall payoff function

The overall payoff function is expressed in Eq. (5), considering how drivers trade off their speed advantages and safety concerns by a tradeoff ratio.

$$C_{\mathrm{M}}(\mathbb{M}, \mathbb{F}) = \mathrm{VoS}_{\mathrm{M}} \cdot \left[V_{\mathrm{M}}(\mathbb{M}, \mathbb{F}) + \psi_{\mathrm{M}} S_{\mathrm{M}}(\mathbb{M}, \mathbb{F})\right] + \varepsilon_{\mathrm{M}} \tag{5a}$$

$$C_{\mathrm{F}}(\mathbb{F}, \mathbb{M}) = \mathrm{VoS}_{\mathrm{F}} \cdot \left[V_{\mathrm{F}}(\mathbb{F}, \mathbb{M}) + \psi_{\mathrm{F}} S_{\mathrm{F}}(\mathbb{F}, \mathbb{M})\right] + \varepsilon_{\mathrm{F}} \tag{5b}$$

where $C_{\mathrm{M}}(\mathbb{M}, \mathbb{F})$ is the payoff of Vehicle M when Vehicle M selects from the strategy set $\mathbb{M}$ while Vehicle F chooses from $\mathbb{F}$ and $C_{\mathrm{F}}(\mathbb{F}, \mathbb{M})$ is the payoff of Vehicle F. VoS is the vehicle's value of speed that can be derived from the value of time (VoT) by assuming the trip distance which maintains the speed benefit, $V_{\mathrm{M}}(\mathbb{M}, \mathbb{F})$ and $V_{\mathrm{F}}(\mathbb{F}, \mathbb{M})$ are the speed benefits with the reference to the baseline scenario, $S_{\mathrm{M}}(\mathbb{M}, \mathbb{F})$ and $S_{\mathrm{F}}(\mathbb{F}, \mathbb{M})$ are the safety costs estimated by proximity and severity of potential collision risk, $\varepsilon_{\mathrm{M}}$ and $\varepsilon_{\mathrm{F}}$ are random terms following a normal distribution to capture the unobserved internal (for example, human's risk compensation behavior to avoid fatigue or boredom Fuller, 2005) and external (such as road geometry and conditions Bobermin et al., 2021) effects, and $\psi_{\mathrm{M}}$ and $\psi_{\mathrm{F}}$ are the trade-off ratios between speed benefits and safety costs:

$$\psi = (\text{Value of Statistical Life (VSL)})/(\text{Value of Speed (VoS)}) \tag{6}$$

**Table 3**
Payoff matrix and micro-based solution conditions of two-player LC games without pricing.

| | | F | |
|---|---|---|---|
| | | Not Yield ($q$) | Yield ($1-q$) |
| M | Change lanes ($p$) | $C_M(c,n),\ C_F(n,c)$ | $C_M(c,y),\ C_F(y,c)$ |
| | Stay ($1-p$) | $C_M(s,n),\ C_F(n,s)$ | $C_M(s,y),\ C_F(y,s)$ |

Note that the driver payoff we estimate here is a kind of benefit, which needs to be maximized for optimization purposes. Then, $\psi$ should be negative because the safety cost is a disutility. Table 3 presents the payoffs of all strategy pairs.

## 3. Two-player LC pricing game

Consistent with assumptions and game settings described in Section 2, we now charge drivers on their 'change lanes' strategies in dense traffic conditions. Vehicle M should pay tolls (denoted as $\tau_P$) for the intended lane changes. At the same time, we compensate Vehicle F who suffers the delay induced by lane changes by $\tau_R$. Consider a set of commuters who are identified by unique IDs. The LC pricing scheme should charge for each game pair (demonstrated as $k$ in the following). Thus, we introduce two pricing schemes from local-optimal (LO) and global-optimal (GO) perspectives. Because the Nash Equilibrium (NE) solution fails to consider the social benefits, the LO (focusing on the local coordination) and the GO (focusing on global densities) pricing schemes are applied for the 'greater good' conditions for all drivers involved.

### *3.1. Local-optimal pricing*

After establishing the base model, we first assess the solutions through both the Nash Equilibrium (NE) and the Local Optimum (LO) from the microscopic scale. For NE, it is proved that at least one feasible solution set exists in finite games (Nash et al., 1950).

The NE indicates a strategy set such that no player can change strategy to obtain a higher expected payoff whatever the player's opponents choose. The expressions of optimal probabilities $(p^*, q^*)$ in the two-player two-strategy NE are:

$$\begin{aligned} &E_M(p^*, q^*) \geq E_M(p, q^*) \\ &E_F(p^*, q^*) \geq E_F(p^*, q) \end{aligned} \tag{7}$$

$$\begin{aligned} &E_M(p,q) = p \cdot \left[q \cdot C_M(c,n) + (1-q) \cdot C_M(c,y)\right] + (1-p) \cdot \left[q \cdot C_M(s,n) + (1-q) \cdot C_M(s,y)\right] \\ &E_F(p,q) = q \cdot \left[p \cdot C_F(n,c) + (1-p) \cdot C_F(n,s)\right] + (1-q) \cdot \left[p \cdot C_F(y,c) + (1-p) \cdot C_F(y,s)\right] \end{aligned} \tag{8}$$

There may be multiple Nash Equilibria, which could be difficult to find the entire set of solutions (Liu et al., 2007). Therefore, we solve this game by the Lemke–Howson complementary pivoting algorithm, which searches at least one strategy set of Nash Equilibria (Lemke and Howson, 1964). Given a $2 \times 2$ payoff matrix $A$ and $B$ in our game, $\Phi_1 \in \mathbb{R}^2$ and $\Phi_2 \in \mathbb{R}^2$ are two best-response polytopes. A pivot operation allows dropping labels with some adjacent labels until the vertices are fully labeled and finally obtaining the NE solution.

Meanwhile, we follow the Pareto Optimality as the local-optimal (LO) solution to develop satisfaction for both agents without making anyone's situation worse off (Censor, 1977). Every game was proved to have at least one Pareto effective point associated with NE solutions (Zhukovskiy and Kudryavtsev, 2016). The pareto-optimal strategy then needs to be selected from the observer's viewpoint that expects social merit, which can be expressed as:

$$\sum_{z \in \mathrm{M,F}} E_z(p^o, q^o) \geq \sum_{z \in \mathrm{M,F}} E_z(p, q) \tag{9}$$

The potential social gap between LO and NE solutions has been revealed in Ji and Levinson (2020b), which is similar to the well-known 'price of anarchy' problem studied in route choice models (Roughgarden, 2005). There are two possible cases occurring in LC maneuvers. Case 1 indicates a situation in which the safety cost is quite small, and in which the spacing between two vehicles ('dilemma-free distance') is adequate to safely engage in aggressive behavior. Thus, there is no social dilemma in this state.

In Case 2, the NE and the LO solutions start to separate, which means a social dilemma emerges. In this scenario, it requires one of the players to 'sacrifice' its own gain to consider the group's total benefit. Otherwise, Vehicle M will have a high probability of changing lanes, and Vehicle F will also have a great probability of not yielding, which may impose a high social cost. See Appendix for numerical examples.

We want no such conflicts, but it is impossible to always maintain the low-risk 'dilemma-free distance' between every two vehicles, especially in some heavy-traffic regimes. Hence, we incentivize the players to eliminate the dilemma and exploit a micro-based LC pricing to coordinate NE and LO solution sets.

In that case, players can make effect to achieve Pareto Optimality. For this, we develop a local-optimal (LO) pricing for LC games. A new payoff matrix and solutions with a pricing term are then constructed as Table 4.

When given a penalty $\tau_{P,k}$ and a reward $\tau_{R,k}$ in game $k$, the game structure/rule can be optimized, and it becomes reasonably fair for rational players. That is, Vehicles M and F can easily reach the consensus for the win-win outcome by the LO pricing. In

**Table 4**
Payoff matrix and solution conditions of two-player LC games with the pricing term.

| | | F | |
|---|---|---|---|
| | | Not Yield ($q$) | Yield ($(1-q)$) |
| M | Change lanes ($p$) | $C(c,n)-\tau_{P},\ C(n,c)$ | $C(c,y)-\tau_{P},\ C(y,c)+\tau_{R}$ |
| | Stay ($1-p$) | $C(s,n),\ C(n,s)$ | $C(s,y),\ C(y,s)+\tau_{R}$ |
| | Solution 1 | Nash Equilibrium $(p^{*},\ q^{*})$ | Local Optimum $(p^{o},\ q^{o})$ |
| | 2 | Nash Equilibrium $(p^{*},\ q^{*})$ | Global Optimum $(p',\ q')$ |

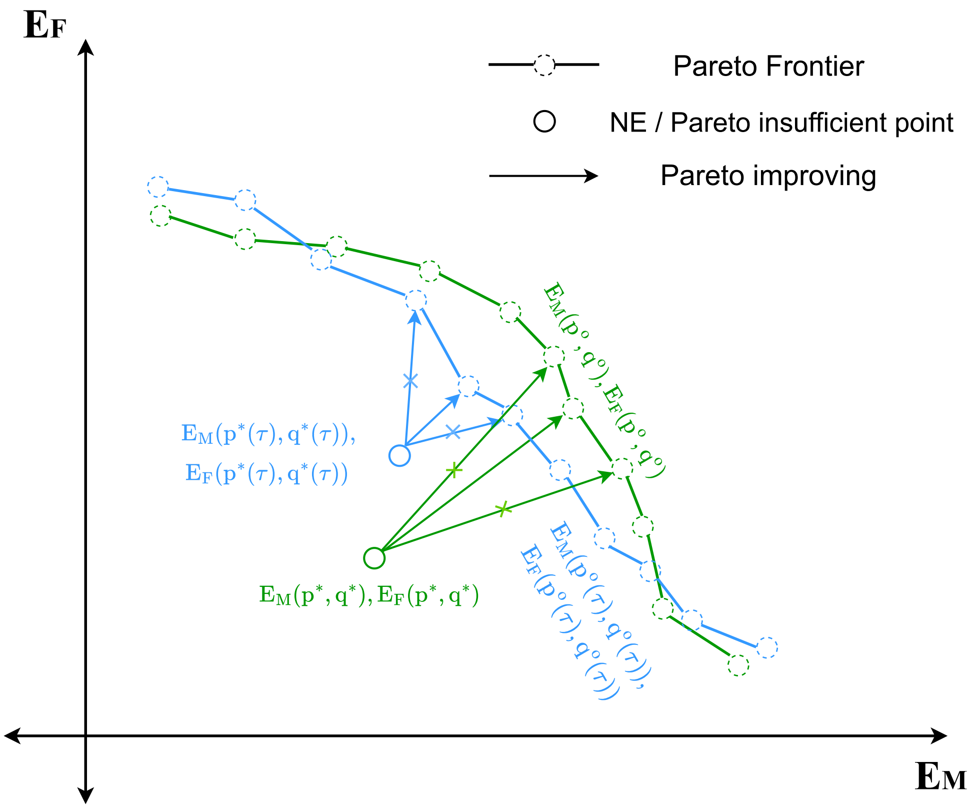


**Fig. 2.** An example for the Pareto frontier and NE/LO solutions with the LO pricing (green: the case without $\tau$, blue: the case with $\tau$).

Fig. 2, all LO solutions are on the Pareto frontier (linked by the blue line). The Pareto frontier can be computed by the $\epsilon$-constraints method (Mavrotas, 2009), which optimizes one of the objectives using other objectives as constraints:

$$\begin{aligned} & E_{\mathrm{M}}(p^{o},q^{o})/E_{\mathrm{F}}(p^{o},q^{o}) = \operatorname{argmax}\ E_{\mathrm{M}}(p,q)/E_{\mathrm{F}}(p,q) \\ & \text{s.t. } E_{\mathrm{F}}(p,q)/E_{\mathrm{M}}(p,q) \geq e \end{aligned} \tag{10}$$

With different sets of the LO, the Pareto frontier and the NE solution (the red point) change accordingly. Finally, we can modify the NE to become/approximate one of the solutions on the Pareto frontier with minimal effort.

Therefore, we can then obtain the expressions of the NE point and its nearest point on the Pareto frontier and then find the appropriate value of pricing to minimize their differences. We solve this non-linear optimization problem with a least-square process for the $k$th game:

$$(\tau^{o}_{\mathrm{P},k}, \tau^{o}_{\mathrm{R},k}) = \underset{\tau_{\mathrm{P},k};\tau_{\mathrm{R},k}}{\operatorname{argmin}} \Big[ \big(E_{\mathrm{M}}\big(p^{o}_{k}(\tau_{\mathrm{P},k}, \tau_{\mathrm{R},k}), q^{o}_{k}(\tau_{\mathrm{P},k}, \tau_{\mathrm{R},k})\big) - E_{\mathrm{M}}\big(p^{*}_{k}(\tau_{\mathrm{P},k}, \tau_{\mathrm{R},k}), q^{*}_{k}(\tau_{\mathrm{P},k}, \tau_{\mathrm{R},k})\big)\big)^{2} \\ + \big(E_{\mathrm{F}}\big(p^{o}_{k}(\tau_{\mathrm{P},k}, \tau_{\mathrm{R},k}), q^{o}_{k}(\tau_{\mathrm{P},k}, \tau_{\mathrm{R},k})\big) - E_{\mathrm{F}}\big(p^{*}_{k}(\tau_{\mathrm{P},k}, \tau_{\mathrm{R},k}), q^{*}_{k}(\tau_{\mathrm{P},k}, \tau_{\mathrm{R},k})\big)\big)^{2} \Big] \\ \text{subject to} \quad \tau_{\mathrm{P},k}, \tau_{\mathrm{R},k} \geq 0 \tag{11}$$

### 3.2. Global-optimal pricing

At the macroscopic scale, a bi-level optimization process is designed to achieve lane-balancing for the whole section. The upper level requires Vehicle M to balance the lane density by filling the less crowded lane to alleviate traffic oscillations, thereby minimizing the total system cost. The lower level seeks individual-optimal solutions of M and F under the lane-balancing rules, giving way to social-good lane changes but blocking selfish behavior. Assume $p'$ is the global-optimal LC probability for any Vehicle M (here we only consider the pure strategy for the consequences, that is, the probability of changing lanes will be either 0% or 100%). In this scenario, we aim to minimize the deviations of the number of vehicles per lane in the whole section, which provides an optimal strategy set $P'$ for each lane:

$$P'_{i} = \underset{P_i}{\operatorname{argmin}} \sum_{i=1}^{I} \left( N_i(P_i) - \overline{N} \right)^{2} \\ p_{(i,i\pm1)}, p_{(i\pm1,i)} \subset P_i \quad \text{for every M changing from/to Lane } i \tag{12}$$

in which $i$ is the lane ID from the rightmost Lane 1 to the leftmost Lane $I$, $N_i$ is the number of vehicles in Lane $i$; $\overline{N}$ is the average number of all vehicles in all lanes, and $p'_{(i,i\pm1)}/p'_{(i\pm1,i)}$ is the global-optimal strategy set for Vehicle M changing from/to Lane $i$.

If given an optimal LC probability $p'_k$ for Vehicle M in game pair $k$, in the lower-level process, Vehicle F will adopt the strategy probability $q'_k$ to maximize the individual payoff. Finally, the optimal strategy probability set $Q'$ for all lag vehicles can be computed. Therefore, in the system, a corresponding strategy combination $(P', Q')$ contributes to the system efficiency through the lane-balancing control.

$$q'_k = \underset{q_k}{\operatorname{argmax}} \left[ E_{\mathrm{F}}(p'_k, q_k) \right] \quad \text{for every } q_k \text{ in } Q \tag{13}$$

Based on this rule, the optimal vehicle counts in each lane can be determined, allowing changes to under-utilized lanes and penalizing lane changes to over-crowded lanes.

However, most drivers may not make decisions as expected by planners. In contrast, they focus on their individual, short-term benefits. As mentioned before, we exploit NE strategy sets to simulate the individually-rational choices of drivers. By comparing NE and GO solutions, we find gaps between them, which should be considered when micro-tolls are applied.

Similarly, we align drivers' preferences with their GO behaviors considering charges for people changing from low-density to high-density lanes. With this toll, we can adjust the NE set $(P^*, Q^*)$ to approximate the GO set $(P', Q')$. In other words, the payoff expectations of NE and GO feasible strategy sets should be minimized. We compute the global-optimal pricing with a least-square optimization for all games ($k$ from 1 to $K$) simultaneously:

$$(\tau'_{\mathrm{P}}, \tau'_{\mathrm{R}}) = \underset{\tau_{\mathrm{P}};\tau_{\mathrm{R}}}{\operatorname{argmin}} \sum_{k=1}^{K} \left[ E_{\mathrm{M}}\big(p'_k(\tau_{\mathrm{P}}, \tau_{\mathrm{R}}), q'_k(\tau_{\mathrm{P}}, \tau_{\mathrm{R}})\big) - E_{\mathrm{M}}\big(p^{*}_k(\tau_{\mathrm{P}}, \tau_{\mathrm{R}}), q^{*}_k(\tau_{\mathrm{P}}, \tau_{\mathrm{R}})\big) \right]^{2} \\ + \sum_{k=1}^{K} \left[ E_{\mathrm{F}}\big(p'_k(\tau_{\mathrm{P}}, \tau_{\mathrm{R}}), q'_k(\tau_{\mathrm{P}}, \tau_{\mathrm{R}})\big) - E_{\mathrm{F}}\big(p^{*}_k(\tau_{\mathrm{P}}, \tau_{\mathrm{R}}), q^{*}_k(\tau_{\mathrm{P}}, \tau_{\mathrm{R}})\big) \right]^{2} \\ \text{subject to} \quad \text{Eq. (12)} \\ \text{Eq. (13)} \\ \tau_{\mathrm{P}}, \tau_{\mathrm{R}} \geq 0 \tag{14}$$

Different from the LO pricing that is time and space varying based on local conditions, the GO micro-toll is equal for drivers who change lanes at the same time and road section.

Unlike cordon- or area-based schemes for congestion pricing, the LO pricing is event-based rather than place determined, and the GO pricing is condition-sensitive. Both require recording every time there are significant changes in the lateral positions of vehicles.

Next, we will compare these two pricing methods in microsimulation experiments and check their respective impacts on the whole system.

## 4. Simulation experiments

### 4.1. Data description

To apply the proposed micro-tolling of lane changing, we first need to calibrate the model and consequently integrate it within microsimulation software. This study uses the real-world data from the Next Generation Simulation (NGSIM) datasets (Colyar and

Halkias, 2007) for model calibration. The NGSIM data comprise two US highways: US-101 and I-80. Each of them collected 45-minute trajectory data in peak hours, including vehicle information such as speeds and locations with a 0.1-second resolution. The lane allocation is similar in the two locations (five one-directional mainline lanes and an auxiliary lane), except for a high-occupancy vehicle (HOV) lane in the I-80 highway.

For both sites, we omit lane changes from or to the auxiliary or HOV lane and only consider those that happen between two normal lanes for discretionary lane changes (DLC). Meanwhile, we only consider the interactions between passenger cars, so cases involving motorcycles or trucks are dropped.

The start and the end of LC games may be indeterminate with the available trajectory data, but the conditions when drivers make decisions (at the game start) and the duration are vital to construct the game. Thus, we follow the rules in Yang et al. (2019) to extract LC trajectories.

To simplify the analysis, we only select single lane changes rather than continuous changes (with the short interval $\leq$ 5 s between two lane changes) in case the previous lane change(s) may have a significant short-term influence on the subsequent one. Lane changes that happen between two main lanes are categorized as DLC, while those changing from (to) the auxiliary lane are considered as MLC. Lane changes that intend to exit the highway starting from middle lanes are regarded as MLC as well. This classification may misclassify some lane changes due to the lack of drivers' route plans or intentions in the trajectory data. All the single DLCs (1,125 samples) are collected for the following analysis. The duration of extracted lane changes is $4.76 \pm 2.42$ s with the range of $[1.1, 13.8]$.

However, it is much more difficult to capture the 'stay' behavior than 'change lanes', because drivers' intention is unavailable from trajectory data. Related research has considered this challenging problem by some simplifications (Talebpour et al., 2015; Kang and Rakha, 2017; Ali et al., 2019, 2021). In this paper, it is assumed the entire period before the LC execution belongs to the 'stay' behavior, and may be terminated at every decision time interval (for example, every 0.1 s) according to surrounding conditions.

We also need to analyze the vehicle driving behind in the target or receiving lane also known as the lag vehicle F. Vehicle F may choose to cooperate or not with Vehicle M. In this model, two strategies are assumed for Vehicle F according to its average acceleration rate within the selected time window when it responds to the intended merging behavior. Some drivers are unwilling to give the passing priority to others so they decide to close the gap by accelerating. Otherwise, they yield involuntarily or voluntarily.

### *4.2. Model calibration and validation*

There are seven parameters ($\beta_{11}$, $\beta_{12}$, $\beta_{21}$, $\beta_{22}$, $\beta_{31}$, $R$, and $\psi$) in the proposed GT model, i.e. Eqs. (1)–(3), that need to be calibrated with real data. Additionally, it is also necessary to validate the model by its predictive performance.

This study introduces a new parameter $\psi$ to measure how people trade-off speed efficiency (represented by the value of speed) and safety (assessed by the value of statistical life) while driving. Also, the cases including both 'change lane' and 'stay' strategies are necessary to be considered for the consistency in the decision-making of Vehicle M. Finally, the driver utility is quantified into real values for the pricing analysis.

In the first step, we use 70% of trajectory data from two respective highways (US-101 and I-80) and compare their calibration results. We first find the Nash Equilibrium solution by the Lemke–Howson algorithm (Lemke and Howson, 1964). The outcomes are presented in the form of mixed strategy probabilities according to specific conditions.

In the next step, parameters are estimated by Sequential Quadratic Programming (SQP) to minimize the errors between observations and predictions for strategy combinations (Liu et al., 2007; Kang and Rakha, 2017; Ali et al., 2019), as:

$$
\begin{aligned}
&(\beta^*, \psi^*, R^*) = \min \sum_{k=1}^{K} L_k(\beta, \psi, R) \\
&L_{\mathrm{k}} = \begin{cases} 0 & \text{if} \quad \hat{\mathbb{M}}_{\mathrm{k}} = \mathbb{M}_{\mathrm{k}}, \hat{\mathbb{F}}_{\mathrm{k}} = \mathbb{F}_{\mathrm{k}} \\ 1 & \text{otherwise} \end{cases}
\end{aligned}
\tag{15}
$$

where $(\beta^*, \psi^*, R^*)$ are calibrated model parameters with the minimum squared errors, in which $\beta^*$ includes the estimates of $\beta_{11}$, $\beta_{12}$, $\beta_{21}$, $\beta_{22}$, $\beta_{31}$, $k$ is the pair ID from 1 to K of all LC games in the whole dataset, $L_k$ denotes the indicator of model prediction, which equals 0 when predicting correctly for both M and F's actions and equals 1 when predicting wrongly, $\hat{\mathbb{M}}$ and $\mathbb{M}$ are predicted and observed strategies of M, and $\hat{\mathbb{F}}$ and $\mathbb{F}$ are predicted and observed strategies of F.

The final estimation outcomes are presented in Table 5. It is found that the magnitudes and signs of the parameters are similar in the two datasets, ensuring the consistency of model application in different road sections. The fitting errors, measured by the Mean Absolute Error (MAE) and the Root Mean Square Error (RMSE), are comparable to other related studies (Kita, 1999; Liu et al., 2007; Talebpour et al., 2015; Ali et al., 2018), revealing this model can capture 86.3% and 87.1% of driver LC behaviors in US-101 and I-80.

From calibration results, the value of $R$ (1.981 s for US-101 and 1.698 s for I-80) corresponds to the average response time of drivers in reality, which falls in a reasonable range. $\beta_{11}$ and $\beta_{21}$ are negative in both datasets. That means the perceived speed advantage of changing lanes or not yielding is less than the actual benefit obtained by drivers. This effect implies that people are effectively more altruistic in reality than the model's objective rationality assumption implies.

The estimated values of $\psi$ are −7,172 and −8,051 in US-101 and I-80, respectively. To interpret how drivers in NGSIM trade-off risks and benefits, the sensitivity to the value of time and trip distance is tested for the magnitude of VSL (the willingness to pay in order to save QALYs), comparing to the VSL recommendations of some studies (for example, 1.2 to 3.8 million US dollars

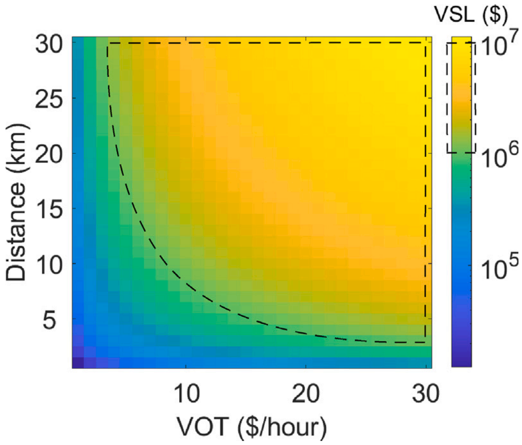


**Fig. 3.** The estimated value of statistical life (VSL) in US dollars with different speed-advantageous distances and value of time (VOT) (the fan-shaped area represents the recommended values by previous VSL studies).

**Table 5**
Calibrated parameters in the GT-based model (70% of data).

| Parameter | $\beta_{11}$ | $\beta_{12}$ | $\beta_{21}$ | $\beta_{22}$ | $\beta_{31}$ | $R$ | $\psi(\times 10^3)$ | MAE | RMSE |
|---|---|---|---|---|---|---|---|---|---|
| US-101 | −4.065 | 7.610 | −1.624 | 5.027 | 8.429 | 1.981 | −7.172 | 0.137 | 0.393 |
| I-80 | −5.902 | 6.557 | −1.351 | 4.528 | 9.634 | 1.698 | −8.051 | 0.129 | 0.372 |

**Table 6**
Validation results between model predictions and actual observations (30% of data).

| Dataset | Behavior | Correct prediction | Observation | Detection rate |
|---|---|---|---|---|
| US-101 | Change lanes | 490 | 622 | 78.78% |
| | Stay | 3,938 | 4,428 | 88.93% |
| | Not yield | 1,147 | 1,415 | 81.06% |
| | Yield | 3,089 | 3,635 | 84.98% |
| | Overall accuracy | 4,401 | 5,050 | 87.15% |
| I-80 | Change lanes | 461 | 598 | 77.09% |
| | Stay | 3,310 | 3,669 | 90.22% |
| | Not yield | 805 | 1,010 | 79.70% |
| | Yield | 2,802 | 3,257 | 86.03% |
| | Overall accuracy | 3,773 | 4,267 | 88.42% |

in Viscusi, 1993, 11.8 million US dollars in the newly-updated report in U.S. Department of Transportation, 2021, 3.2 to 6.7 million CAD in Dionne and Lanoie, 2004, and around 2 million pounds suggested by Treasury, 2018). The acceptable ranges of those two parameters are shown in Fig. 3, corresponding to US dollars.

After that, we substitute the calibrated parameters into the model and validate the model with the remaining 30% of data not included in model calibration. Note that this study obtained an unsatisfying error level in terms of individual strategies, consistent with the related studies. It is believed that delivering the accuracy results for individual strategies to exhibit the model performance is also important. In addition to the strategy prediction accuracy, we provide validation results based on the vehicle-to-vehicle strategy pair in Table 6 (in Overall Accuracy). Finally, over 87% of total cases can be correctly predicted for the pairwise behaviors of M and F in the two datasets, indicating satisfactory accuracy of the GTLC model.

### 4.3. Microsimulation tests

We assume a 640-m road section with an on-ramp and an off-ramp. The vehicle mass is assumed to follow the distribution $\mathcal{N}(1400, 200^2)$ in kilograms, and the vehicle length is assumed to be 6.0 m for all vehicles. The LC game interaction will be triggered when the distance between two vehicles is less than 50 m. Due to no route preferences designed in this model, Vehicle M will always compete with the one close to M in potential target (receiving) lanes when both of them enter the interaction range. Note that we apply the same model parameters calibrated from the naturalistic driving data to the microsimulation (Kim and Mahmassani, 2011). Meanwhile, we test scenarios with different traffic demands (low demand: 1,000 veh/h/ln, medium demand: 1,500 veh/h/ln, high demand: 2,000 veh/h/ln). The AIMSUN MicroAPI realizes all the newly designed rules in the simulation.

The overall control process is presented in Algorithm 1. Vehicles are assumed to adopt the Gipps' model to follow their leaders and change lanes when not getting involved in LC games. However, once they trigger the lane-changing interaction, the game theory-based LC controller overtakes as the new movement-updating rule. At each time step, the controlled vehicles obtain local or global traffic information and update the speed choice and the lane selection for the next tick.

**Algorithm 1:** Game Theory Controller

**Input:** Simulation environment parameters, model parameters $\beta_{11}$, $\beta_{12}$, $\beta_{21}$, $\beta_{22}$, $\beta_{31}$, average response time $R$, trade-off ratio $\psi$
**Output:** Strategies and updated speeds of M and F

- **for** *Every time step* **do**
  - Find all vehicle IDs in the main lanes and record their position and speed information
  - **if** $\Delta x_{\mathrm{MF}} < 50\,m$ **then**
    - **for** *Every subject vehicle M* **do**
      - Find its opponent vehicle F and lead vehicle L and obtain their current information
      - Calculate their payoffs for all different strategy combinations
      - Solve the game with the mixed Nash Equilibrium by the Lemke–Howson algorithm
      - Get $p^*$, $q^*$
      - **while** *Payoff expectation differences $\Delta E$ are converged* **do**
        - **if** *Micro-based pricing rules* **then**
          - Solve the game with the Pareto Optimality $(p^{\mathrm{o}}, q^{\mathrm{o}})$ (Eq. (11))
          - Deploy pricing schemes $(\tau_{\mathrm{P}}^{\mathrm{o}}, \tau_{\mathrm{R}}^{\mathrm{o}})$
          - Align $E_{\mathrm{M}}^{\mathrm{o}}$ and $E_{\mathrm{F}}^{\mathrm{o}}$ with the NE
        - **else if** *Macro-based pricing rules* **then**
          - **Top level:** Solve the game with the global density-balancing rule $(P', Q')$ (Eq. (14))
          - **Bottom level:** Select pairwise global-optimal strategy $(p', q')$
          - Deploy pricing schemes $(\tau_{\mathrm{P}}', \tau_{\mathrm{R}}')$
          - Align $E_{\mathrm{M}}'$ and $E_{\mathrm{F}}'$ with the NE
      - If converged, get $p(\tau)$, $q(\tau)$ for the final strategy probabilities
      - Randomization: Generate two random values $p_{\mathrm{d}}$ and $q_{\mathrm{d}}$
      - Decide which strategy M or F selects
      - Update the speed $v$ and the lane selection for the next tick according to the selected strategies
  - **else**
    - Update the speed $v$ and the lane selection for the next tick according to the Gipps' CF model

## 5. Results

The microsimulation is run with the time step of 0.8 s after a warm-up period of 60 s. The total simulation takes 30 min. We repeat this process ten times with different random seeds and report the average of those outcomes.

In the following, we hypothesize that, under the pricing controls, drivers tend to minimize the probability of choosing LC strategies when unnecessary. The total delay is accumulated over time caused by inappropriate lane changes, increasing the travel time spent. Conflicts are also reduced by those pricing schemes, detected by the surrogate safety assessment model (SSAM) by FHWA (Pu et al., 2008). Finally, we check the system revenue by aggregating the total penalties and rewards assigned to drivers. Three types of simulations, including the tests without (W/O) pricing, with local-optimal (LO) pricing, and with global-optimal (GO) pricing, are performed. The simulation results of speed contours, the number of lane changes, the total travel time, the number of conflicts, and pricing values are presented in Figs. 4, 5, 7, and 8.

### *5.1. Number of lane changes*

In the following, we present the results with high- and medium-demand conditions in which pricing leads to significant improvements in Figs. 5(a) and 5(b). Drivers' naturalistic LC behaviors are simulated based on the Nash Equilibrium. With the pricing term, the number of lane changes is significantly reduced by 26.5% with LO and 6.2% with GO in the high-demand situation. That means lane changers will reconsider their behaviors with a potential penalty or reward. The LO eliminates more lane changes than the GO to achieve local optimization, while the GO encourages LC behavior to smooth the traffic flow.

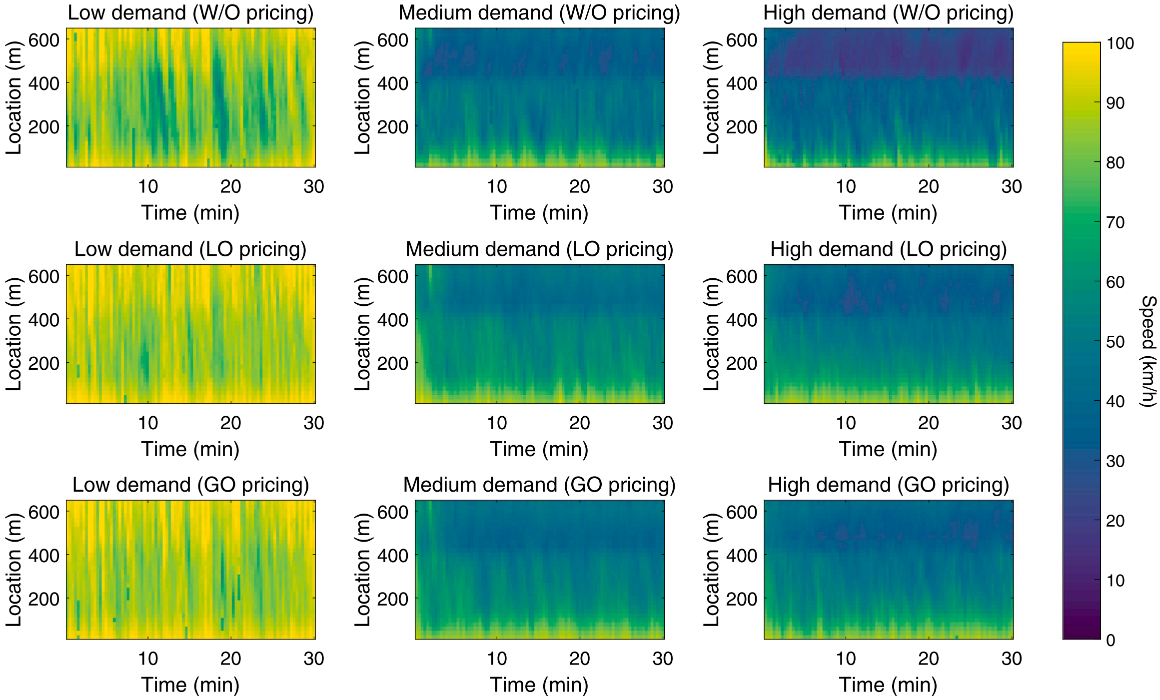


**Fig. 4.** The speed contours of the road section (from top to bottom: scenarios without pricing, with local-optimal pricing, and with global-optimal pricing; from left to right: scenarios with low-demand (1,000 veh/h/ln), medium-demand (1,500 veh/h/ln), and high-demand (2,000 veh/h/ln)).

## 5.2. Total travel time and delay

We check the efficiency of the proposed LC pricing by total travel time (TTT) under different controls. It is found that, in the over-saturated traffic, the LO and GO schemes diminish the impact of aggressive LC behaviors and reduce the system overall travel time by 20.1% and 24.3%, respectively. However, this effect appears not to be significant in medium-demand situations shown in Fig. 5(d).

The delay time series in the high-demand scenario is shown in Fig. 6, indicating the GO pricing eliminates more delay than the LO pricing.

## 5.3. Number of conflicts

The results above indicate the flow efficiency, tracing the disruptions caused by excessive lane changes and the mitigating effect of pricing schemes. From the perspective of safety, we count the number of conflicts, an essential indicator in safety assessments, by vehicle trajectories. The occurrence of conflicts is sensitive to the model parameter settings in simulation experiments, so with the same experiment settings, we compare different levels of conflicts among three scenarios (without pricing, with local-optimal pricing, and with global-optimal pricing). We consider a TTC threshold of 1.5 s and a PET threshold of 5.0 s for the conflict criterion.

In the medium-demand condition, 61.6% and 40.0% of conflicts on average are reduced by the LO and GO respectively (shown in Fig. 5(f)). Furthermore, in Fig. 5(e), the LO and GO can significantly eliminate 81.5% and 83.4% of conflicts in the congested situation. In addition, we also find that the LO pricing scheme leads to a slightly narrower range of conflict numbers [22,54] than the GO [21,60]. The reason is, with GO, all lane changers share the same charge at the same time interval, whose punishment strength is insufficient for strong aggressors. Thus, they are still willing to take risks, resulting in more conflicts.

## 5.4. Pricing and revenue

We demonstrate the value of micro-tolls by its percentages in different value ranges. Fig. 7 shows penalties and rewards in the high-demand situation for the LO prices that vary for different game pairs. Fig. 8 illustrates the GO prices for all potential lane changers at the same tick. Values of the LO are mostly higher than the GO. We also notice, some values of LO appear to be quite significant (1–2 $). That means Vehicle M may decide to change lanes in some extremely risky situations where F has to stop and yield in case of a collision. It is worth imposing a strict punishment on such risk-taking lane changers.

Compared to the LO, the micro-toll amount of GO keeps a relatively low value. Besides, it significantly improves the road utilization and reduces the system delay. However, the pricing of GO may be too high for some locally beneficial lane changes

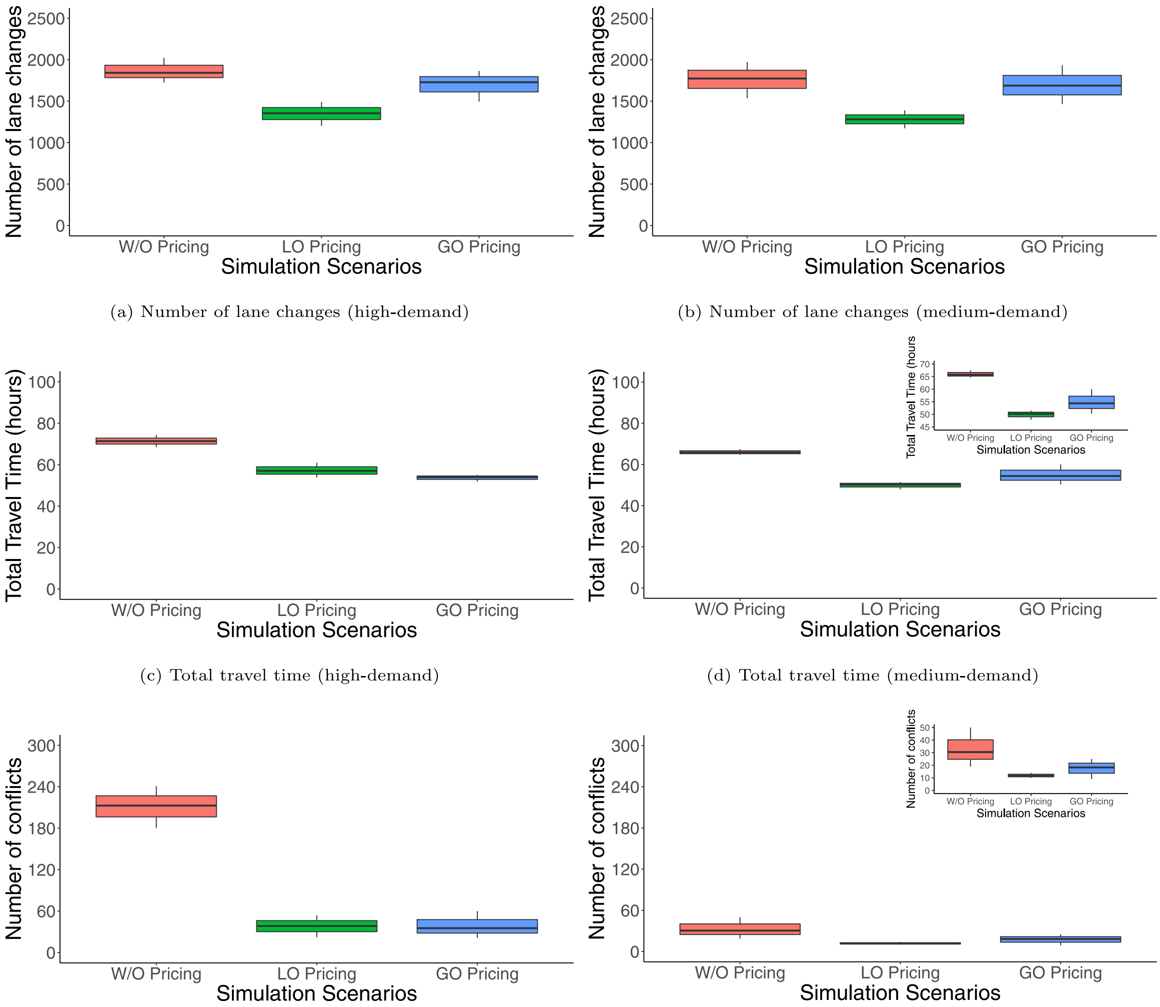


(a) Number of lane changes (high-demand)

(b) Number of lane changes (medium-demand)

(c) Total travel time (high-demand)

(d) Total travel time (medium-demand)

(e) Number of conflicts (high-demand)

(f) Number of conflicts (medium-demand)

**Fig. 5.** The simulation result comparison between high-demand and medium-demand conditions.

**Table 7**
System total values of penalties, rewards, and net revenues in two pricing rules.

| Values ($) | LO pricing | | | GO pricing | | |
|---|---|---|---|---|---|---|
| Scenarios | $\sum \tau_P$ | $\sum \tau_R$ | $\Delta\tau$ | $\sum \tau_P$ | $\sum \tau_R$ | $\Delta\tau$ |
| High-demand | 1091.47 | 558.06 | 533.40 | 702.03 | 515.76 | 186.27 |
| Medium-demand | 645.58 | 390.44 | 255.14 | 268.43 | 181.50 | 86.93 |
| Low-demand | 203.73 | 66.61 | 137.12 | 79.11 | 52.40 | 26.71 |

that are not captured by lane-balancing rules. For example, drivers may change lanes to leave space for others who drive faster, even from the low-density to the high-density lane, which is not favorable under GO. At the same time, its high tolls would not be sufficiently punitive for aggressors to diminish their likelihood of changing lanes.

We then check the whole system's revenues after the micro-pricing implementation, counting all penalties and rewards. For the two micro-pricing schemes, the net revenues ($\Delta\tau$) during the 30-minute process are positive (as listed in Table 7), indicating the whole pricing system is self-liquidating, so that no subsidies are needed externally.

It is recommended to deploy the GO type initially due to its relatively simple and cost-effective approach using existing traffic sensors, and broadcasting that information to all vehicles. The LO type of pricing requires more detailed data provided by in-vehicle sensors, as are coming with new vehicle technologies (Davis et al., 2020), but will produce more precise tolls that account for local conditions, and may be able to be deployed in years to come. Other pricing strategies may also be developed over time.

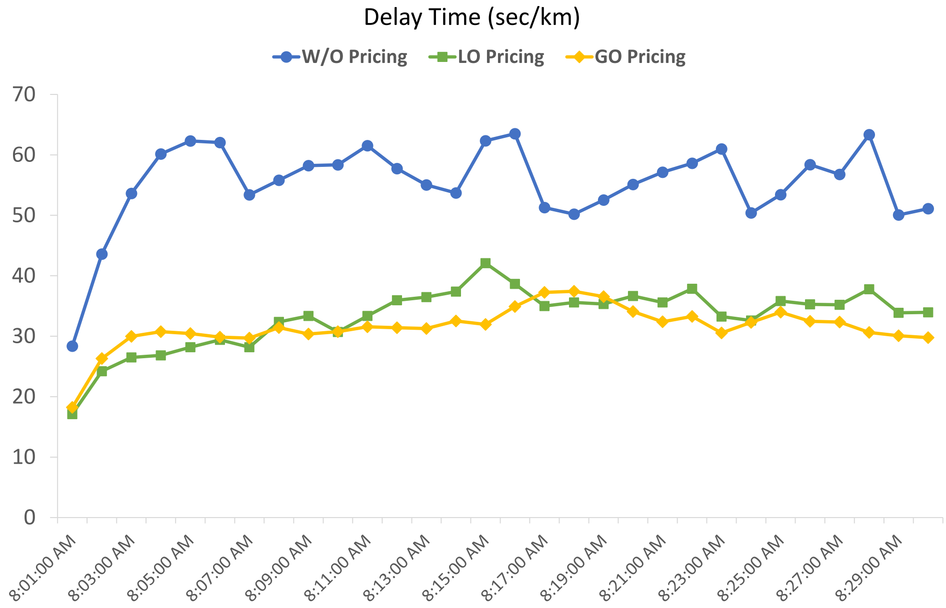


**Fig. 6.** The average delay over time in the high-demand scenario.

## 6. Conclusions

Due to the low cost, drivers over-consume self-interested lane changes compared to the social optimal way. Those behaviors result in significant system delays for other road users (not only for their opponents in competitions but for vehicles who get delayed because of LC-caused local oscillations) and excess crash risk. Social welfare would improve if LC drivers internalized the cost for the delay suffered by others and compensate for what they impose because of their aggressive behaviors. Therefore, we have designed the pricing policy to regulate drivers' selfish decisions in LC maneuvers.

This paper first analyzes drivers' interactions in LC maneuvers under the game-theoretic framework and constructs payoff functions to reveal how drivers trade-off efficiency and safety. Then, we propose micro- and macro-based pricing schemes to coordinate strategies adopted by drivers, and their performance is validated through the replicated real-world scenario in simulation experiments. The results indicate the two tested pricing schemes can reduce the total travel time and improve the safety level of the system. The locally optimal (LO) scheme focuses on penalizing individual aggressive behaviors (especially for extremely dangerous actions), while the globally optimal (GO) scheme aims to balance lane densities to increase the overall road utility. However, the LO ignores the importance of system coordination, and the GO fails to judge behaviors at the level of maneuvers and over-emphasizes lane balancing especially in uncongested conditions.

We conclude that the LO scheme performs better in significantly reducing aggressive and unsafe lane changes. The LO scheme imposes much heavier charges and rewards on more aggressive behaviors and considers less significant restrictions on less risky actions. Unlike LO, the GO scheme penalizes lane changes that aggravate the congestion in over-crowded lanes, but is likely simpler to implement.

In terms of their implementation in real-world scenarios, the GO pricing covers overall traffic conditions while the LO pricing observes local interactions. The LO pricing acts as an alternative to manage lane changes locally using more detailed local data. There may, for instance, be a toll for every lane change that increases system congestion or risk. This kind of vehicle-based pricing system relies on innovative technologies such as vehicular on-board units (Clements et al., 2020) and vehicular communications (Basar and Cetin, 2017).

The proposed pricing model can be easily extended to deal with different individuals based on their value of time (VOT) and trade-off ratios, if known to all. It is worth discussing, for example, whether vehicles with low VOT (e.g. a single occupant car) will or should yield to those with high VOT (e.g. a bus) or the opposite, and how pricing facilitates that transaction.

Meanwhile, autonomous vehicles are able to rapidly and accurately recognize surrounding information and make corresponding decisions with high-quality detection methods and short response time. The automation of vehicles is expected to provide the potential for intelligent lane coordination within the scope of the proposed micro-pricing scheme.

Increasing the number of lanes and players modeled is a logical extension. Each extra lane and extra player may significantly increase the degree of complexity. Future datasets are expected to provide route planning data of vehicles for improving the reliability of model results. Meanwhile, one may investigate the impact of interactions between trucks, passenger cars, or vehicles with different lengths on pricing in following studies. Also, the assumptions of complete information and rationality may limit the scope of the LC pricing application, which can be addressed by considering Bayesian games (Shao et al., 2020) and bounded rationality (Wang et al., 2022). In addition, we should also realize that successful pricing implementation will need strong government administration and public compliance to overcome the political challenges.

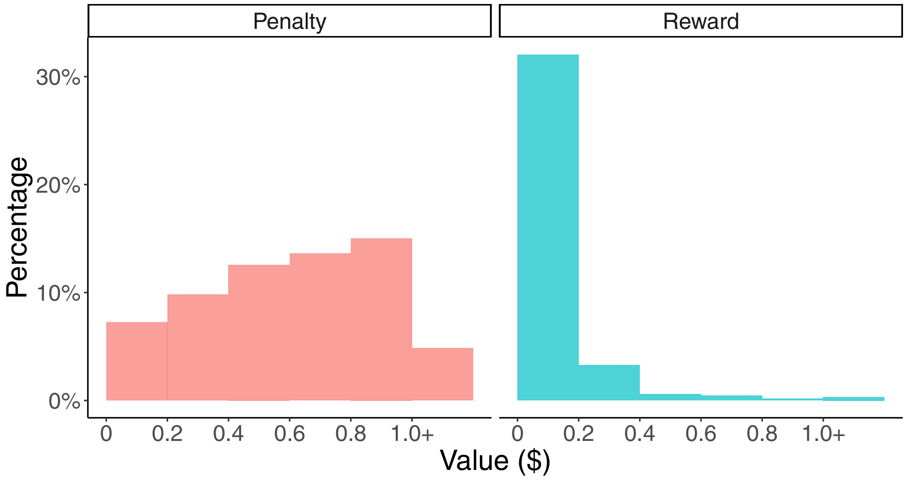


**Fig. 7.** Pricing values of the LO in the high-demand scenario.

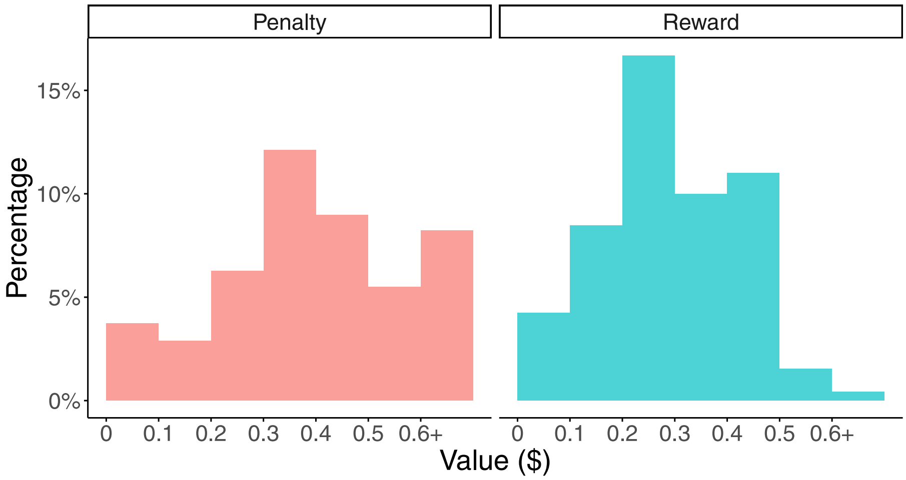


**Fig. 8.** Pricing values of the GO in the high-demand scenario.

## CRediT authorship contribution statement

**Ang Ji:** Conceptualization, Methodology, Software, Validation, Formal analysis, Investigation, Writing – original draft. **Mohsen Ramezani:** Methodology, Writing – review & editing, Supervision. **David Levinson:** Conceptualization, Writing – review & editing, Supervision.

## Appendix. Possible payoff outcomes of two representative cases with pure Nash Equilibrium solution(s)

In a less congested scenario (Case 1), the non-cooperative behaviors ('Change lane' and 'Not yield') induce minimal safety costs due to the large distances between vehicles. Therefore, both players in the LC game are willing to trade off little potential collision risk to save more travel time. In the end, they achieve the maximum individual benefits as well as their maximum total payoffs (see Table A.1).

However, in a high-density situation (Case 2), the safety costs become significant. Each of the players would expect others' yielding behavior while behaving selfishly to grab personal payoffs as many as possible. Finally, they get into the 'lose-lose' consequence where neither of the players intends to give way to the opponent. For the sake of cooperation, players should negotiate an agreement that one needs to 'sacrifice' part of individual gains to ensure social-good outcomes.

**Table A.1**
Possible payoff outcomes of two representative cases with pure Nash Equilibrium solution(s).

Case 1

| | | F | |
|---|---|---|---|
| | | Not Yield ($q$) | Yield ($1-q$) |
| M | Change lane ($p$) | **10, 10** * | 8, 3 |
| | Stay ($1-p$) | 4, 8 | 4, 5 |

Case 2

| | | F | |
|---|---|---|---|
| | | Not Yield ($q$) | Yield ($1-q$) |
| M | Change lane ($p$) | **2, 2** * | **10, 5** |
| | Stay ($1-p$) | **6, 10** | 6, 6 |

## References


Ali, Y., Zheng, Z., Haque, M.M., 2018. Connectivity's impact on mandatory lane-changing behaviour: Evidences from a driving simulator study. Transp. Res. C 93, 292–309.

Ali, Y., Zheng, Z., Haque, M.M., Wang, M., 2019. A game theory-based approach for modelling mandatory lane-changing behaviour in a connected environment. Transp. Res. C 106, 220–242.

Ali, Y., Zheng, Z., Haque, M.M., Yildirimoglu, M., Washington, S., 2021. CLACD: A complete Lane-Changing decision modeling framework for the connected and traditional environments. Transp. Res. C 128, 103162.

Basar, G., Cetin, M., 2017. Auction-based tolling systems in a connected and automated vehicles environment: Public opinion and implications for toll revenue and capacity utilization. Transp. Res. C 81, 268–285.

Bell, M.G., 2000. A game theory approach to measuring the performance reliability of transport networks. Transp. Res. B 34 (6), 533–545.

Bobermin, M.P., Silva, M.M., Ferreira, S., 2021. Driving simulators to evaluate road geometric design effects on driver behaviour: A systematic review. Accid. Anal. Prev. 150, 105923.

Cassidy, M.J., Rudjanakanoknad, J., 2005. Increasing the capacity of an isolated merge by metering its on-ramp. Transp. Res. B 39 (10), 896–913.

Censor, Y., 1977. Pareto optimality in multiobjective problems. Appl. Math. Optim. 4 (1), 41–59.

Chen, H., Lam, J.S.L., Liu, N., 2018. Strategic investment in enhancing port–hinterland container transportation network resilience: A network game theory approach. Transp. Res. B 111, 83–112.

Clements, L.M., Kockelman, K.M., Alexander, W., 2020. Technologies for congestion pricing. Res. Transp. Econ. 100863.

Coifman, B., Mishalani, R., Wang, C., Krishnamurthy, S., 2006. Impact of lane-change maneuvers on congested freeway segment delays: Pilot study. Transp. Res. Rec. 1965 (1), 152–159.

Colyar, J., Halkias, J., 2007. US Highway Dataset. Federal Highway Administration (FHWA). Tech. Rep. FHWA-HRT-07-030. 2, 4, 5.

Cortés-Berrueco, L.E., Gershenson, C., Stephens, C.R., 2016. Traffic games: modeling freeway traffic with game theory. PLoS One 11 (11), e0165381.

Davis, B., Ji, A., Liu, B., Levinson, D., 2020. Moving array traffic probes. Front. Future Transp. 2.

Dionne, G., Lanoie, P., 2004. Public choice about the value of a statistical life for cost-benefit analyses: The case of road safety. J. Transp. Econ. Policy (JTEP) 38 (2), 247–274.

Fisk, C., 1984. Game theory and transportation systems modelling. Transp. Res. B 18 (4–5), 301–313.

Fuller, R., 2005. Towards a general theory of driver behaviour. Accid. Anal. Prev. 37 (3), 461–472.

Gettman, D., Pu, L., Sayed, T., Shelby, S.G., Energy, S., et al., 2008. Surrogate Safety Assessment Model and Validation. Tech. Rep. FHWA-HRT-08-051, Turner-Fairbank Highway Research Center, Federal Highway Administration, United States.

Gipps, P.G., 1986. A model for the structure of lane-changing decisions. Transp. Res. B 20 (5), 403–414.

He, J., Qu, J., Zhang, J., He, Z., 2022. The impact of a single discretionary lane change on surrounding traffic: An analytic investigation. IEEE Trans. Intell. Transp. Syst..

Hidas, P., 2005. Modelling vehicle interactions in microscopic simulation of merging and weaving. Transp. Res. C 13 (1), 37–62.

Iwamura, Y., Tanimoto, J., 2018. Complex traffic flow that allows as well as hampers lane-changing intrinsically contains social-dilemma structures. J. Stat. Mech. Theory Exp. 2018.

Ji, A., Levinson, D., 2020a. An energy loss-based vehicular injury severity model. Accid. Anal. Prev. 146, 105730.

Ji, A., Levinson, D., 2020b. Estimating the social Gap with a game theory model of lane changing. IEEE Trans. Intell. Transp. Syst. 22 (10), 6320–6329.

Ji, A., Levinson, D., 2020c. A review of game theory models of lane changing. Transp. A Transp. Sci. 16 (3), 1628–1647.

Ji, A., Ramezani, M., Levinson, D., 2022. Joint modeling of longitudinal and lateral dynamics in lane-changing maneuvers. Transp. B Transp. Dynam. http://dx.doi.org/10.1080/21680566.2022.2154717.

Jin, W., 2010. A kinematic wave theory of lane-changing traffic flow. Transp. Res. B 44 (8–9), 1001–1021.

Jula, H., Kosmatopoulos, E.B., Ioannou, P.A., 2000. Collision avoidance analysis for lane changing and merging. IEEE Trans. Veh. Technol. 49 (6), 2295–2308.

Kang, K., Rakha, H.A., 2017. Game theoretical approach to model decision making for merging maneuvers at freeway on-ramps. Transp. Res. Rec. 2623 (1), 19–28.

Kang, K., Rakha, H.A., 2018. Modeling driver merging behavior: A repeated game theoretical approach. Transp. Res. Rec. 2672 (20), 144–153.

Kim, J., Mahmassani, H.S., 2011. Correlated parameters in driving behavior models: Car-following example and implications for traffic microsimulation. Transp. Res. Rec. 2249 (1), 62–77.

Kita, H., 1999. A merging–giveway interaction model of cars in a merging section: a game theoretic analysis. Transp. Res. A Policy Pract. 33 (3–4), 305–312.

Laureshyn, A., Ceunynck, T.D., Karlsson, C., Svensson, Å., Daniels, S., 2017. In search of the severity dimension of traffic events: Extended Delta-V as a traffic conflict indicator. Accid. Anal. Prev. 98, 46–56.

Laval, J.A., Daganzo, C.F., 2006. Lane-changing in traffic streams. Transp. Res. B 40 (3), 251–264.

Lemke, C.E., Howson, Jr., J.T., 1964. Equilibrium points of bimatrix games. J. Soc. Ind. Appl. Math. 12 (2), 413–423.

Levinson, D., 2005. Micro-foundations of congestion and pricing: A game theory perspective. Transp. Res. A Policy Pract. 39 (7–9), 691–704.

Li, M., Li, Z., Xu, C., Liu, T., 2020. Short-term prediction of safety and operation impacts of lane changes in oscillations with empirical vehicle trajectories. Accid. Anal. Prev. 135, 105345.
Lighthill, M.J., Whitham, G.B., 1955. On kinematic waves II. A theory of traffic flow on long crowded roads. Proc. R. Soc. Lond. Ser. A Math. Phys. Sci. 229 (1178), 317–345.
Lin, D., Li, L., Jabari, S.E., 2019. Pay to change lanes: A cooperative lane-changing strategy for connected/automated driving. Transp. Res. C 105, 550–564.
Littlechild, S.C., Thompson, G., 1977. Aircraft landing fees: a game theory approach. Bell J. Econ. 186–204.
Liu, H.X., Xin, W., Adam, Z., Ban, J., 2007. A game theoretical approach for modelling merging and yielding behaviour at freeway on-ramp sections. Transp. Traffic Theory 3, 197–211.
Lou, Y., Yin, Y., Laval, J.A., 2011. Optimal dynamic pricing strategies for high-occupancy/toll lanes. Transp. Res. C 19 (1), 64–74.
Mauch, M., Cassidy, M.J., 2002. Freeway traffic oscillations: observations and predictions. In: Transportation and Traffic Theory in the 21st Century: Proceedings of the 15th International Symposium on Transportation and Traffic Theory, Adelaide, Australia, 16-18 July 2002. Emerald Group Publishing Limited, pp. 653–673.
Mavrotas, G., 2009. Effective implementation of the $\epsilon$-constraint method in multi-objective mathematical programming problems. Appl. Math. Comput. 213 (2), 455–465.
Nash, J.F., et al., 1950. Equilibrium points in N-person games. Proc. Natl. Acad. Sci. 36 (1), 48–49.
National Highway Traffic Safety Administration, 2021. Traffic Safety Facts 2019: a Compilation of Motor Vehicle Crash Data. Tech. Rep. DOT HS 813 141, United States.
Nowak, M.A., 2006. Five rules for the evolution of cooperation. Science 314 (5805), 1560–1563.
Pande, A., Abdel-Aty, M., 2006. Assessment of freeway traffic parameters leading to lane-change related collisions. Accid. Anal. Prev. 38 (5), 936–948.
Patire, A.D., Cassidy, M.J., 2011. Lane changing patterns of bane and benefit: Observations of an uphill expressway. Transp. Res. B 45 (4), 656–666.
Pu, L., Joshi, R., Energy, S., et al., 2008. Surrogate Safety Assessment Model (SSAM)–Software User Manual. Tech. Rep. FHWA-HRT-08-050, Turner-Fairbank Highway Research Center.
Ramezani, M., Ye, E., 2019. Lane density optimisation of automated vehicles for highway congestion control. Transp. B Transp. Dynam. 7 (1), 1096–1116.
Richards, P.I., 1956. Shock waves on the highway. Oper. Res. 4 (1), 42–51.
Roughgarden, T., 2005. Selfish Routing and the Price of Anarchy. Vol. 174. MIT press Cambridge.
Shao, H., Zhang, M., Feng, T., Dong, Y., 2020. A discretionary lane-changing decision-making mechanism incorporating drivers' heterogeneity: A signalling game-based approach. J. Adv. Transp. 2020.
Sobhani, A., Young, W., Logan, D., Bahrololoom, S., 2011. A kinetic energy model of two-vehicle crash injury severity. Accid. Anal. Prev. 43 (3), 741–754.
Society of Automotive Engineers, 2015. Operational Definitions of Driving Performance Measures and Statistics. Tech. Rep. J2944, Warrendale, PA: Society of Automotive Engineers.
Spicer, R., Miller, T., 2010. Final Report to the National Highway Traffic Safety Administration: Uncertainty Analysis of Quality Adjusted Life Years Lost. Pacific Institute for Research and Evaluation (PIRE), Calverton, MD.
Talebpour, A., Mahmassani, H.S., Hamdar, S.H., 2015. Modeling lane-changing behavior in a connected environment: A game theory approach. Transp. Res. C 59, 216–232.
Toledo, T., Koutsopoulos, H.N., Ben-Akiva, M.E., 2003. Modeling integrated lane-changing behavior. Transp. Res. Rec. 1857 (1), 30–38.
Treasury, H., 2018. The Green Book: Central Government Guidance on Appraisal and Evaluation. OGL Press, London, UK.
U.S. Department of Transportation, 2021. Departmental guidance on valuation of a statistical life in economic analysis. https://www.transportation.gov/office-policy/transportation-policy/revised-departmental-guidance-on-valuation-of-a-statistical-life-in-economic-analysis.
Viscusi, W.K., 1993. The value of risks to life and health. J. Econ. Lit. 31 (4), 1912–1946.
Von Neumann, J., Morgenstern, O., 1944. Theory of Games and Economic Behavior. Princeton University Press.
Wang, M., Hoogendoorn, S.P., Daamen, W., van Arem, B., Happee, R., 2015. Game theoretic approach for predictive lane-changing and car-following control. Transp. Res. C 58, 73–92.
Wang, B., Li, Z., Wang, S., Li, M., Ji, A., 2022. Modeling bounded rationality in discretionary lane change with the quantal response equilibrium of game theory. Transp. Res. B 164, 145–161.
Yang, M., Wang, X., Quddus, M., 2019. Examining lane change gap acceptance, duration and impact using naturalistic driving data. Transp. Res. C 104, 317–331.
Zhukovskiy, V.I., Kudryavtsev, K.N., 2016. Pareto-optimal Nash equilibrium: Sufficient conditions and existence in mixed strategies. Autom. Remote Control 77 (8), 1500–1510.
Zimmermann, M., Schopf, D., Lütteken, N., Liu, Z., Storost, K., Baumann, M., Happee, R., Bengler, K.J., 2018. Carrot and stick: A game-theoretic approach to motivate cooperative driving through social interaction. Transp. Res. C 88, 159–175.